Dalton Transactions

ROYAL SOCIETY OF CHEMISTRY

COMMUNICATION

View Article Online
View Journal | View Issue

Cite this: *Dalton Trans.*, 2024, **53**, 13320

Received 13th June 2024,
Accepted 24th July 2024

DOI: 10.1039/d4dt01729c

rsc.li/dalton

Reticular chemistry guided single-linker constructed pillar-layered metal–organic frameworks *via* an *in situ* "one-pot" strategy†

Zhen-Sha Ma,[a,b] Hui Yang,[b] Kai Xing,[c] Kang Zhou,[b] Gonghao Lu *[a] and Xiao-Yuan Liu *[b]

In the present work, we report a "two-in-one" strategy to construct single-linker-based pillar-layered metal–organic frameworks (PL-MOFs) guided by reticular chemistry *via* an *in situ* "one-pot" approach. Two carboxyl groups and one pyridine group are integrated into one molecular skeleton to form bifunctional organic linkers *via* the reaction of pyridine-containing aldehyde and bicarboxylate-containing *o*-phenylenediamine. During the synthesis of organic linkers, two zinc-based PL-MOFs, non-interpenetrated HIAM-3016-op and two-fold interpenetrated HIAM-3017-op, can be simultaneously constructed. The different interpenetrations for these two PL-MOFs can be attributed to the increased length of the pyridine-containing moiety. HIAM-3017-op can be utilized for $Cr_2O_7^{2-}$ detection with excellent sensitivity and selectivity. The present work not only provides a novel insight to design and prepare PL-MOFs with specific structures guided by reticular chemistry, but also indicates the universality of the *in situ* "one-pot" strategy to construct porous materials.

As one of the subgroups of metal–organic frameworks (MOFs), pillar-layered MOFs (PL-MOFs)[1,2] have received considerable attention due to their unique structures and potential applications in sensing,[3] catalysis[4–6] and gas separation.[7] The most important feature of PL-MOFs is the presence of two linkers in one MOF, which can offer more possibility to tune the structures and properties of the resultant MOFs. Usually, the 2D layer in PL-MOFs is formed *via* the connection of metal sites and carboxylate groups from ditopic-,[3,8,9] tritopic-[4] or tetratopic[10–14]-type carboxylate acid to generate a binuclear "paddle-wheel" $M_2(COO)_4$ (M = Zn, Co, Cd) type structure, whereas the pillaring linkers are coordinated to the unsaturated metal sites *via* nitrogen atoms as shown in Scheme 1a. Owing to the nature that the two linkers are orderly distributed in the whole structure, PL-MOFs have been considered as some of the ideal platforms to study the energy transfer with highly tunable absorption and emission spectral overlap between the pillar linkers and the linkers in the layer, in which one acts as the energy donor and the other is the energy acceptor.[9,11,13–16]

Although a number of PL-MOFs have been reported, compared with non-pillar 3D MOFs, drawbacks such as low porosity and low stability of the structures have limited more specific investigations in this area due to the structural flexibility.[8,17,18] Therefore, it is essential to design new structures with special linkers to improve the thermal and chemical stability without decreasing the void volume of the whole framework. In recent years, the development of reticular chemistry[19–21] has facilitated the discovery of MOFs with unprecedented structures.[22–28] It has been successfully proven that reticular chemistry can provide helpful guidelines for the top-down design and precise construction of MOFs, in which organic and inorganic building units can be rationally designed at the atom level.[29–33] Given the underlying nets, the geometrical constrains and the specific functions of organic and inorganic building units,[34–36] MOFs with desired structures and enhanced performances have been constructed *via* the guidance of reticular chemistry.[37–40]

On the other hand, for the construction of MOFs, the conventional method is to use pre-synthesized organic linkers to react with inorganic units, where extensive and time-consuming organic synthesis has to be performed. To avoid these shortcomings, an *in situ* "one-pot" strategy has been developed to facilely prepare MOFs, where *in situ* organic synthesis and MOF construction simultaneously happen under the same

[a]*School of Chemical Engineering, University of Science and Technology Liaoning, 185 Qianshan Zhong Road, Anshan 114051, P. R. China. E-mail: ghlu@ustl.edu.cn*
[b]*Hoffmann Institute of Advanced Materials, Shenzhen Polytechnic University, 7098 Liuxian Blvd, Nanshan District, Shenzhen 518055, P. R. China. E-mail: liuxiaoyuan1989@szpt.edu.cn*
[c]*Department of Chemistry, College of Basic Medicine, Third Military Medical University (Army Medical University), Chongqing, 400038, P. R. China. E-mail: kaixing@tmmu.edu.cn*

†Electronic supplementary information (ESI) available. CCDC 2354184, 2354185 and 2368472. For ESI and crystallographic data in CIF or other electronic format see DOI: https://doi.org/10.1039/d4dt01729c

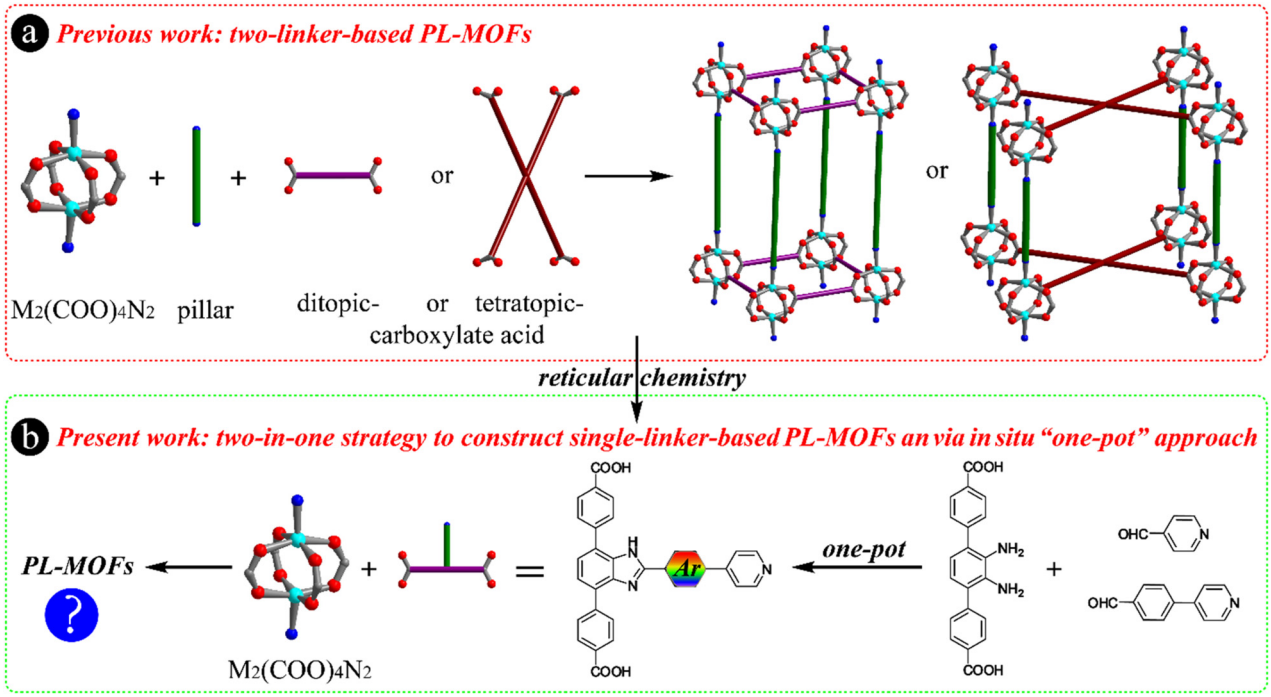

Scheme 1 Schematic diagram illustrating the construction of PL-MOFs by (a) conventional methods using ditopic or tetratopic carboxylate acid and nitrogen-containing molecules as the linkers and (b) the reticular chemistry guided "two-in-one" strategy to construct single-linker-based PL-MOFs *via* an *in situ* "one-pot" approach and the corresponding structures of linkers and precursors.

solvothermal conditions.[41–44] This strategy has been used to successfully prepare MOFs with various structures and applications, especially for Zr-MOFs.

Bearing the unique structural features of PL-MOFs in mind, herein, guided by reticular chemistry,[20,33,45] we envision that a two-in-one strategy might be developed to prepare PL-MOFs using only one kind of organic linker generated *via* an *in situ* "one-pot" strategy. These organic linkers will possess a T-shaped structure containing two carboxylate groups and one pyridine group *via* a reaction between pyridine-containing aldehyde and bicarboxylate-containing *o*-phenylenediamine (Scheme 1b).

To verify our hypothesis, 2′,3′-diamino-[1,1′:4′,1″-terphenyl]-4,4″-dicarboxylic acid (H_2DATC) and isonicotinaldehyde (Fig. 1a) were first chosen as the precursors to synthesize T-shaped 4,4′-(2-(pyridin-4-yl)-1*H*-benzo[*d*]imidazole-4,7-diyl) dibenzoic acid (H_2PBIA), using which the proposed PL-MOFs might be simultaneously constructed. This *in situ* "one-pot" strategy has been successfully used in our previous work to construct a series of Zr-MOFs.[46] A typical synthesis of a single-linker-based PL-Zn-MOF, HIAM-3016-op (HIAM = Hoffmann Institute of Advanced Materials; 30 = zinc), is schematically shown in Fig. 1a and b: a 5 mL vial containing 3.0 mL *N*,*N*-dimethylformamide (DMF), $Zn(NO_3)_3{\cdot}6H_2O$ (0.17 mmol, 49.4 mg), H_2DATC (0.075 mmol, 26.1 mg) and isonicotinaldehyde (0.077 mmol, 8.2 mg) was placed in a preheated oven at 100 °C, and then the colorless single crystals (Fig. S1†) were obtained after 3 days. Single crystal X-ray diffraction (sc-XRD) analysis revealed that HIAM-3016-op is a PL-MOF, which possesses a three-dimensional (3D) structure and crystallizes in the monoclinic crystal system with the *C*2/*c* space group (Table S1,† Fig. 1c and d). The organic linker indeed is H_2PBIA generated *via* the *in situ* reaction between H_2DATC and isonicotinaldehyde (Fig. 1e). H_2PBIA was confirmed *via* the ^{1}H NMR spectrum using the digested HIAM-3016-op (Fig. S2†), which is similar to the directly synthesized H_2PBIA (Fig. S3†). As depicted in Fig. 1c, d and Fig. S4,† each Zn(II) is square-pyramidally coordinated by four carboxylate oxygen atoms from four H_2PBIA linkers at the basal positions and one nitrogen atom from one H_2PBIA linker at the apical position. Two crystallographically equivalent Zn(II) cations are bridged by four carboxylate groups adopting a bis-bidentate coordination mode to generate a dinuclear Zn(II) "paddle-wheel" $Zn_2(COO)_4$ secondary building unit (SBU) (Fig. S5†). These SBUs are linked together by carboxylate groups of H_2PBIA linkers to form a 2D flat layer with square grids. The layer square grids are further connected by the pyridine group from the H_2PBIA linker to form a 3D framework. In order to form 3D PL-MOFs, it should be noted that the angle is 56.94° between the 2D layer and the pyridine-based pillar moiety (Fig. 1d, e and Fig. S6†), which makes the whole structure look like a two-fold interpenetrated framework from the *c* axis (Fig. 1c). The pyridine groups in the whole structure are parallel with each other. Further structural analysis indicates that 3016-op possesses a 2-nodal (3,6)-c net with the point symbol of $\{4^2{\cdot}6\}_2\{4^4{\cdot}6^2{\cdot}8^8{\cdot}10\}$, resulting in an **ant** topology (Fig. 1g). An

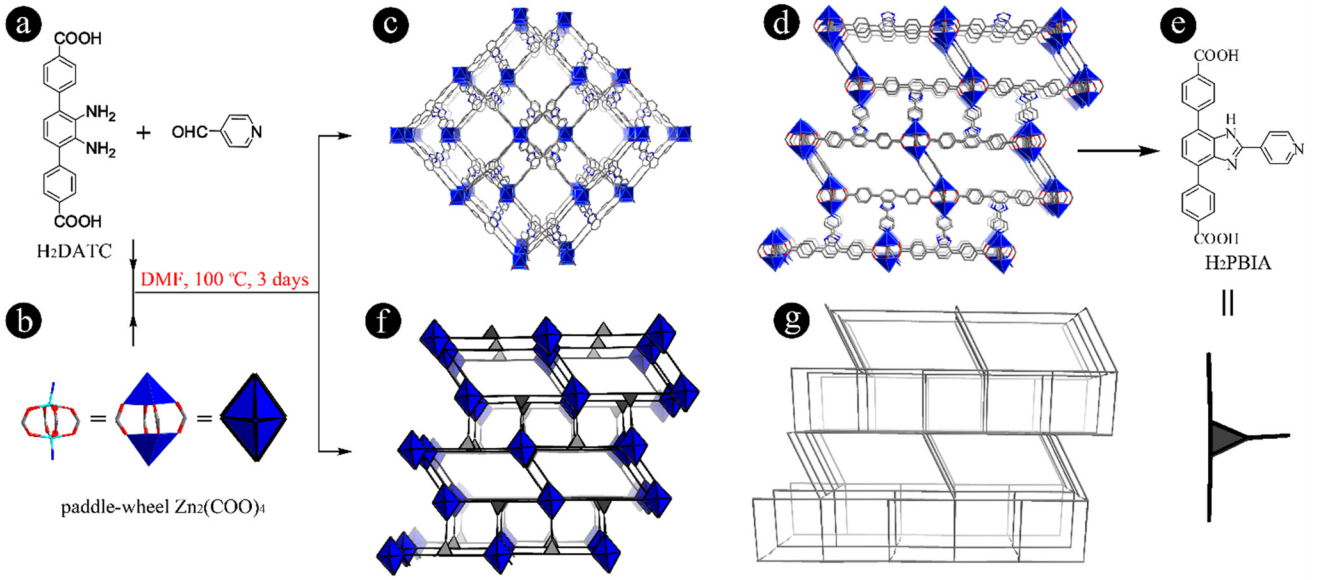

Fig. 1 The molecular structures of H_2DATC and isonicotinaldehyde (a), the structure of paddle-wheel $Zn_2(COO)_4$ (b), the single crystal structure of HIAM-3016-op (c and d), the corresponding linker structure of H_2PBIA (e), and the underlying net of HIAM-3016-op (f and g).

almost same Zn-MOF, HIAM-3016, can be constructed using directly synthesized H_2PBIA under similar solvothermal conditions (Table S2†). The aforementioned results demonstrate that the two-in-one strategy indeed can be utilized to construct PL-MOFs by combining two carboxylate groups and one pyridine group into one organic linker using the *in situ* one-pot approach.

Inspired by the successful construction of single-linker based HIAM-3016-op *via* the *in situ* "one-pot" strategy, we attempted to use different organic precursors to construct various single-linker based PL-MOFs. This investigation will not only confirm the universality of the proposed strategy but also enrich the structural diversity and functionalization of the resultant MOFs. Commercially available 4-(pyridin-4-yl)benzaldehyde was chosen as the pyridine-containing precursor to react with H_2DATC. Using similar synthesis conditions to those for HIAM-3016-op (Fig. 2a and b), large single crystals of HIAM-3017-op were obtained (Fig. S7†). sc-XRD analysis revealed that HIAM-3017-op crystallizes in the monoclinic crystal system with the *C*2/c space group, which is the same as that for HIAM-3016-op. As shown in Fig. 2c, d and S8,† HIAM-3017-op is a PL-MOF constructed using an *in situ* gener-

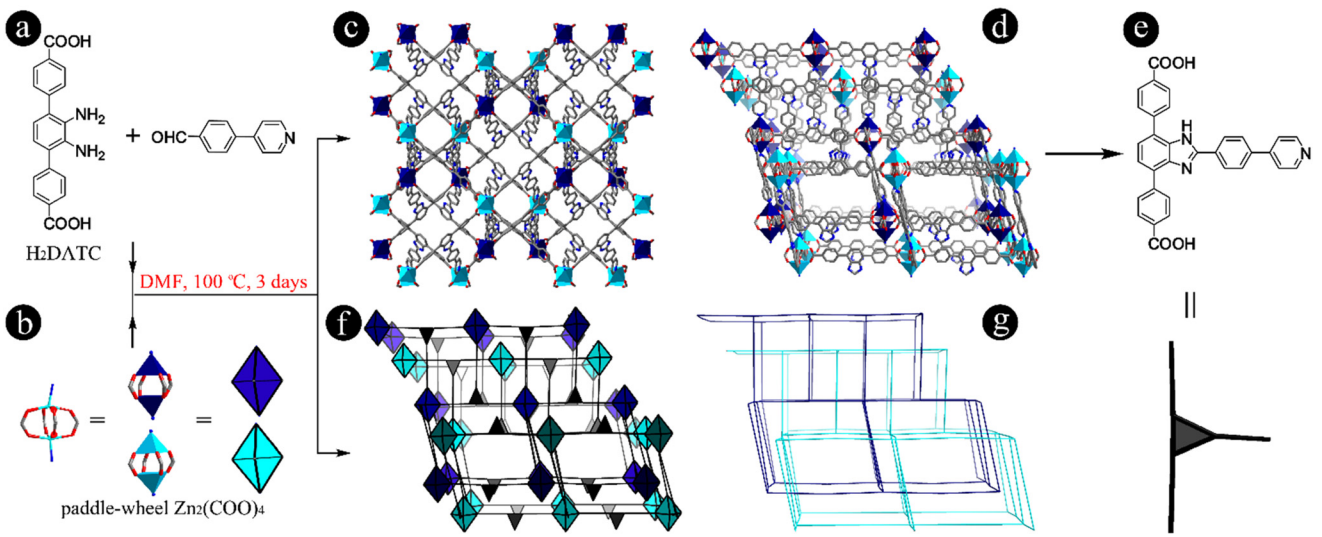

Fig. 2 The molecular structures of H_2DATC and 4-(pyridin-4-yl)benzaldehyde (a), the structure of paddle-wheel $Zn_2(COO)_4$ (b), the single crystal structure of HIAM-3017-op (c and d), the corresponding linker structure of H_2PPBIA (e), and the underlying net of HIAM-3017-op (f and g).

ated linker, 4,4′-(2-(4-(pyridin-4-yl)phenyl)-1*H*-benzo[*d*]imidazole-4,7-diyl)dibenzoic acid (H_2PPBIA) (Fig. 2e), as the organic linker, which was also confirmed *via* the ^{1}H NMR spectrum of digested HIAM-3017-op (Fig. S9†).

In the structure of HIAM-3017-op, two equivalent Zn(II) ions are bridged by four carboxylate groups from four deprotonated H_2PPBIA linkers to form a binuclear "paddle-wheel" $Zn_2(COO)_4$ as the SBU. These SBUs are connected by other carboxylate groups to give (4,4)-c 2D layers, which are further extended by the pyridine-based pillar moiety to form the 3D network. This structural feature is the same as that for HIAM-3016-op. However, the great difference in HIAM-3017-op is that the formed 3D network is interpenetrated to generate a 2-fold framework. In addition, due to the increased length of the pyridine-containing moiety, the angle between the 2D layer and the pyridine-based pillar increased to 81.30° (Fig. S10†). Topological analysis indicated that HIAM-3017-op possesses the same underlying net as HIAM-3016-op (Fig. 2f and g).

The phase purity of HIAM-3016-op and HIAM-3017-op was confirmed by the agreement between simulated and experimental powder X-ray diffraction patterns (PXRD) as shown in Fig. 3a. The solid-state emission and absorption of these two MOFs were also measured. As depicted in Fig. 3b, HIAM-3016-op and HIAM-3017-op exhibit similar optical behaviors with the absorption and emission maxima at 403/485 nm and 384/478 nm, respectively. Then the thermal stability of HIAM-3016-op and HIAM-3017-op was evaluated. Both of them show high thermal stability up to 400 °C as confirmed by thermogravimetric analysis (Fig. S11 and S12†). However, the surface areas of these two MOFs cannot be obtained because their crystallinity cannot be maintained during the activation even using supercritical CO_2 (Fig. S13†). Then we tested the stability of ground HIAM-3017-op and the corresponding optical behavior in aqueous solution to explore its potential application as a chemical sensor. The PXRD patterns of ground HIAM-3017-op matched well with the simulated one even after soaking in water for one day, indicating its mechanical and chemical stability (Fig. 3c and Fig. S14†). The ground HIAM-3017-op exhibited bright emission in aqueous solution with emission maxima at 521 nm, which is 43 nm red-shifted compared with that in the solid state (Fig. 3d).

Then various 200 μM anions (CH_3COO^-, F^-, Cl^-, I^-, HCO_3^-, CO_3^{2-}, IO_4^-, NO_2^-, SO_3^{2-}, SO_4^{2-} and $Cr_2O_7^{2-}$) were separately added to the aqueous solution of ground HIAM-3017-op to evaluate the emission responses to common anions. As shown in Fig. 4a, only $Cr_2O_7^{2-}$ showed remarkable emission quenching with a quenching percentage of 65%. The other ten common anions led to a much lower fluorescence quenching or enhancement effect, indicating that HIAM-3017-op can be used as a highly selective chemical sensor for $Cr_2O_7^{2-}$ detection. A titration experiment was then conducted to determine the sensitivity of HIAM-3017-op toward $Cr_2O_7^{2-}$. The emission intensity of HIAM-3017-op gradually decreased with increasing $Cr_2O_7^{2-}$ concentration (Fig. 4b). According to the Stern–Volmer equation, a linear correlation coefficient of 0.998 was calculated for HIAM-3017-op in the $Cr_2O_7^{2-}$ concentration range from 5 μM to 200 μM (Fig. 4c). Accordingly, the detection limit for $Cr_2O_7^{2-}$ was determined to be 0.63 μM for HIAM-3017-op. The PXRD patterns of HIAM-3017-op after detection well match with those before sensing (Fig. 4d), which confirms the chemical stability of HIAM-3017-op. HIAM-3017-op also exhibited repeatable detection capability for $Cr_2O_7^{2-}$, although decreased quenching efficiencies were observed with values of 65.0%, 62.4% and 47.8% for three

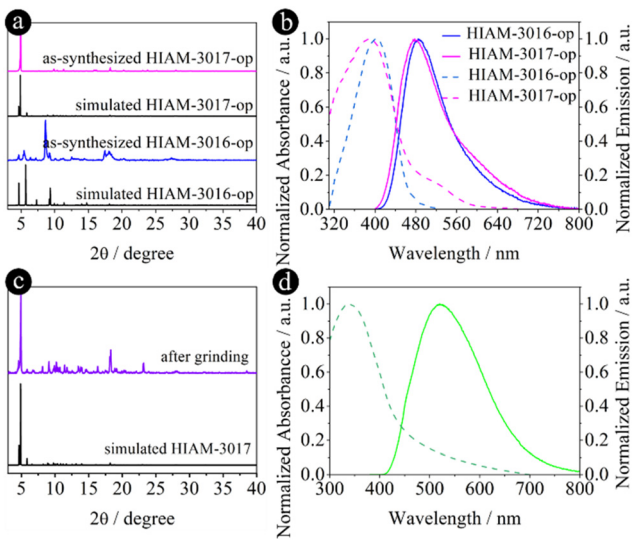

Fig. 3 PXRD patterns of simulated and as-synthesized HIAM-3016-op and HIAM-3017-op (a), the solid-state photoluminescence spectra (solid lines) and UV-vis absorption spectra (dash lines) of HIAM-3016-op and HIAM-3017-op (b), PXRD of HIAM-3017-op after grinding (c), the photoluminescence spectrum (solid line) and UV-vis absorption spectrum (dash line) of HIAM-3017-op in aqueous solution after grinding (d).

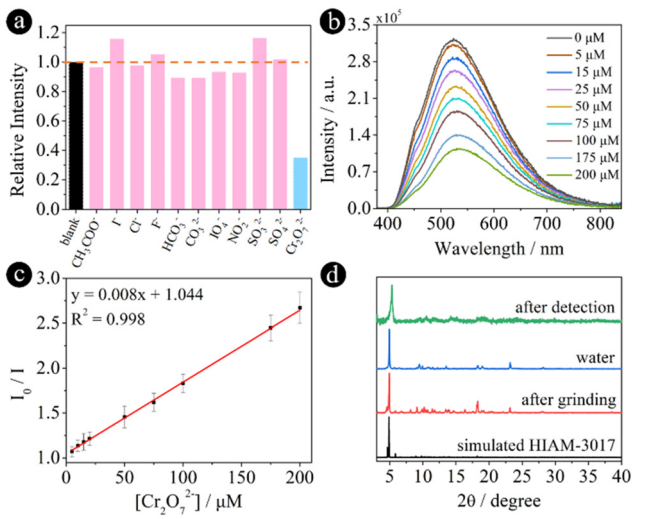

Fig. 4 Selectivity test of HIAM-3017 toward various anions (concentration = 200 μM) (a), $Cr_2O_7^{2-}$ concentration-dependent emission quenching of HIAM-3017 (b), the corresponding Stern–Volmer plot (c), and the PXRD patterns of HIAM-3017 after different treatments (d).

cycles (Fig. S15†). This reduced performance can be attributed to the incomplete removal of $Cr_2O_7^{2-}$ during each cycle and the loss of crystallinity of HIAM-3017-op (Fig. S15†). The aforementioned results demonstrate that HIAM-3017-op can be utilized as a great chemical sensor for $Cr_2O_7^{2-}$ detection with excellent sensitivity, selectivity and high stability.

In conclusion, guided by reticular chemistry, two pillar-layered MOFs, non-interpenetrated HIAM-3016-op and two-fold interpenetrated HIAM-3017-op, are successfully constructed by integrating two carboxylate groups and one pyridine group into one linker skeleton *via* an *in situ* "one-pot" strategy. HIAM-3017-op exhibits high sensitivity and selectivity for $Cr_2O_7^{2-}$ detection. This work provides a new insight for rationally designing organic linkers and discovering new MOFs guided by reticular chemistry *via* an *in situ* "one-pot" strategy.

Data availability

The data that support the findings of this study are available from the corresponding author, upon reasonable request.

Conflicts of interest

There are no conflicts to declare.

Acknowledgements

K. Xing acknowledges the financial support from Chongqing Doctoral "Through Train" Scientific Research Program (No. CSTB2022BSXM-JCX0128). X.-Y. Liu acknowledges the financial support from Shenzhen Science and Technology Program (20231123083040001) and start-up funding for Shenzhen High-Caliber Personnel of Shenzhen Polytechnic University (6022310053K).

References

1 N. C. Burtch and K. S. Walton, *Acc. Chem. Res.*, 2015, **48**, 2850–2857.
2 F. ZareKarizi, M. Joharian and A. Morsali, *J. Mater. Chem. A*, 2018, **6**, 19288–19329.
3 K. Shen, Z. Ju, L. Qin, T. Wang and H. Zheng, *Dyes Pigm.*, 2017, **136**, 515–521.
4 X. Zhang, Y.-Z. Zhang, Y.-Q. Jin, L. Geng, D.-S. Zhang, H. Hu, T. Li, B. Wang and J.-R. Li, *Inorg. Chem.*, 2020, **59**, 11728–11735.
5 F. Cao, M. Zhao, Y. Yu, B. Chen, Y. Huang, J. Yang, X. Cao, Q. Lu, X. Zhang, Z. Zhang, C. Tan and H. Zhang, *J. Am. Chem. Soc.*, 2016, **138**, 6924–6927.
6 Y. Lin, H. Wan, D. Wu, G. Chen, N. Zhang, X. Liu, J. Li, Y. Cao, G. Qiu and R. Ma, *J. Am. Chem. Soc.*, 2020, **142**, 7317–7321.
7 Q. Chen, S. Xian, X. Dong, Y. Liu, H. Wang, D. H. Olson, L. J. Williams, Y. Han, X.-H. Bu and J. Li, *Angew. Chem., Int. Ed.*, 2021, **60**, 10593–10597.
8 Y. Qi, H. Xu, X. Li, B. Tu, Q. Pang, X. Lin, E. Ning and Q. Li, *Chem. Mater.*, 2018, **30**, 5478–5484.
9 H.-L. Xia, K. Zhou, S. Wu, D. Ren, K. Xing, J. Guo, X. Wang, X.-Y. Liu and J. Li, *Chem. Sci.*, 2022, **13**, 8036–8044.
10 O. K. Farha, C. D. Malliakas, M. G. Kanatzidis and J. T. Hupp, *J. Am. Chem. Soc.*, 2010, **132**, 950–952.
11 C. Y. Lee, O. K. Farha, B. J. Hong, A. A. Sarjeant, S. T. Nguyen and J. T. Hupp, *J. Am. Chem. Soc.*, 2011, **133**, 15858–15861.
12 W. Bury, D. Fairen-Jimenez, M. B. Lalonde, R. Q. Snurr, O. K. Farha and J. T. Hupp, *Chem. Mater.*, 2013, **25**, 739–744.
13 D. E. Williams, J. A. Rietman, J. M. Maier, R. Tan, A. B. Greytak, M. D. Smith, J. A. Krause and N. B. Shustova, *J. Am. Chem. Soc.*, 2014, **136**, 11886–11889.
14 E. A. Dolgopolova, D. E. Williams, A. B. Greytak, A. M. Rice, M. D. Smith, J. A. Krause and N. B. Shustova, *Angew. Chem., Int. Ed.*, 2015, **54**, 13639–13643.
15 H.-J. Son, S. Jin, S. Patwardhan, S. J. Wezenberg, N. C. Jeong, M. So, C. E. Wilmer, A. A. Sarjeant, G. C. Schatz, R. Q. Snurr, O. K. Farha, G. P. Wiederrecht and J. T. Hupp, *J. Am. Chem. Soc.*, 2013, **135**, 862–869.
16 W. Danowski, F. Castiglioni, A. S. Sardjan, S. Krause, L. Pfeifer, D. Roke, A. Comotti, W. R. Browne and B. L. Feringa, *J. Am. Chem. Soc.*, 2020, **142**, 9048–9056.
17 G. F. Turner, S. C. McKellar, D. R. Allan, A. K. Cheetham, S. Henke and S. A. Moggach, *Chem. Sci.*, 2021, **12**, 13793–13801.
18 P. Vervoorts, J. Keupp, A. Schneemann, C. L. Hobday, D. Daisenberger, R. A. Fischer, R. Schmid and G. Kieslich, *Angew. Chem., Int. Ed.*, 2021, **60**, 787–793.
19 O. M. Yaghi, M. O'Keeffe, N. W. Ockwig, H. K. Chae, M. Eddaoudi and J. Kim, *Nature*, 2003, **423**, 705–714.
20 N. W. Ockwig, O. Delgado-Friedrichs, M. O'Keeffe and O. M. Yaghi, *Acc. Chem. Res.*, 2005, **38**, 176–182.
21 O. M. Yaghi, M. J. Kalmutzki and C. S. Diercks, *Introduction to Reticular Chemistry*, Wiley, 2019, pp. 1–509.
22 N. R. Catarineu, A. Schoedel, P. Urban, M. B. Morla, C. A. Trickett and O. M. Yaghi, *J. Am. Chem. Soc.*, 2016, **138**, 10826–10829.
23 Z. Chen, Ł. J. Weseliński, K. Adil, Y. Belmabkhout, A. Shkurenko, H. Jiang, P. M. Bhatt, V. Guillerm, E. Dauzon, D.-X. Xue, M. O'Keeffe and M. Eddaoudi, *J. Am. Chem. Soc.*, 2017, **139**, 3265–3274.
24 V. Guillerm, T. Grancha, I. Imaz, J. Juanhuix and D. Maspoch, *J. Am. Chem. Soc.*, 2018, **140**, 10153–10157.
25 Z. Chen, Z. Thiam, A. Shkurenko, L. J. Weselinski, K. Adil, H. Jiang, D. Alezi, A. H. Assen, M. O'Keeffe and M. Eddaoudi, *J. Am. Chem. Soc.*, 2019, **141**, 20480–20489.
26 Y.-F. Zhang, Z.-H. Zhang, L. Ritter, H. Fang, Q. Wang, B. Space, Y.-B. Zhang, D.-X. Xue and J. Bai, *J. Am. Chem. Soc.*, 2021, **143**, 12202–12211.

27 J. Si, H.-L. Xia, K. Zhou, J. Li, K. Xing, J. Miao, J. Zhang, H. Wang, L.-L. Qu, X.-Y. Liu and J. Li, *J. Am. Chem. Soc.*, 2022, **144**, 22170–22177.
28 T. Peng, C.-Q. Han, H.-L. Xia, K. Zhou, J. Zhang, J. Si, L. Wang, J. Miao, F.-A. Guo, H. Wang, L.-L. Qu, G. Xu, J. Li and X.-Y. Liu, *Chem. Sci.*, 2024, **15**, 3174–3181.
29 Z. Chen, S. L. Hanna, L. R. Redfern, D. Alezi, T. Islamoglu and O. K. Farha, *Coord. Chem. Rev.*, 2019, **386**, 32–49.
30 Y. Liu, M. O'Keeffe, M. M. J. Treacy and O. M. Yaghi, *Chem. Soc. Rev.*, 2018, **47**, 4642–4664.
31 Z. Chen, H. Jiang, M. Li, M. O'Keeffe and M. Eddaoudi, *Chem. Rev.*, 2020, **120**, 8039–8065.
32 L. Feng, K.-Y. Wang, X.-L. Lv, T.-H. Yan, J.-R. Li and H.-C. Zhou, *J. Am. Chem. Soc.*, 2020, **142**, 3069–3076.
33 R. Freund, S. Canossa, S. M. Cohen, W. Yan, H. Deng, V. Guillerm, M. Eddaoudi, D. G. Madden, D. Fairen-Jimenez, H. Lyu, L. K. Macreadie, Z. Ji, Y. Zhang, B. Wang, F. Haase, C. Wöll, O. Zaremba, J. Andreo, S. Wuttke and C. S. Diercks, *Angew. Chem., Int. Ed.*, 2021, **60**, 23946–23974.
34 V. Guillerm and D. Maspoch, *J. Am. Chem. Soc.*, 2019, **141**, 16517–16538.
35 H. Jiang, D. Alezi and M. Eddaoudi, *Nat. Rev. Mater.*, 2021, **6**, 466–487.
36 M. J. Kalmutzki, N. Hanikel and O. M. Yaghi, *Sci. Adv.*, 2018, **4**, eaat9180.
37 Z. Chen, P. Li, X. Zhang, P. Li, M. C. Wasson, T. Islamoglu, J. F. Stoddart and O. K. Farha, *J. Am. Chem. Soc.*, 2019, **141**, 2900–2905.
38 C. S. Diercks, Y. Liu, K. E. Cordova and O. M. Yaghi, *Nat. Mater.*, 2018, **17**, 301–307.
39 Z. Chen, P. Li, R. Anderson, X. Wang, X. Zhang, L. Robison, L. R. Redfern, S. Moribe, T. Islamoglu, D. A. Gómez-Gualdrón, T. Yildirim, J. F. Stoddart and O. K. Farha, *Science*, 2020, **368**, 297–303.
40 T. He, X.-J. Kong, J. Zhou, C. Zhao, K. Wang, X.-Q. Wu, X.-L. Lv, G.-R. Si, J.-R. Li and Z.-R. Nie, *J. Am. Chem. Soc.*, 2021, **143**, 9901–9911.
41 X.-J. Kong, T. He, Y.-Z. Zhang, X.-Q. Wu, S.-N. Wang, M.-M. Xu, G.-R. Si and J.-R. Li, *Chem. Sci.*, 2019, **10**, 3949–3955.
42 J. Lyu, X. Zhang, Z. Chen, R. Anderson, X. Wang, M. C. Wasson, P. Bai, X. Guo, T. Islamoglu, D. A. Gómez-Gualdrón and O. K. Farha, *ACS Appl. Mater. Interfaces*, 2019, **11**, 42179–42185.
43 U. S. F. Arrozi, V. Bon, S. Krause, T. Lübken, M. S. Weiss, I. Senkovska and S. Kaskel, *Inorg. Chem.*, 2020, **59**, 350–359.
44 X.-J. Kong, T. He, J. Zhou, C. Zhao, T.-C. Li, X.-Q. Wu, K. Wang and J.-R. Li, *Small*, 2021, **17**, 2005357.
45 M. O'Keeffe, M. A. Peskov, S. J. Ramsden and O. M. Yaghi, *Acc. Chem. Res.*, 2008, **41**, 1782–1789.
46 C.-Q. Han, L. Wang, J. Si, K. Zhou and X.-Y. Liu, *Small*, 2024, **20**, 2402263.